The Solution of the Wave-Diffusion Equation by a Caputo Derivative-Based Finite Element Method Formulation

by

R. M. Corrêa[1], J. A. M. Carrer[2,*], B. S. Solheid[3], J. Trevelyan[4], M. Arndt[1], R. D. Machado[1]

[1]PPGEC: Programa de Pós-Graduação em Engenharia Civil
Universidade Federal do Paraná,
CEP 81531-990, Curitiba, PR, Brasil

[2]PPGMNE: Programa de Pós-Graduação em Métodos Numéricos em Engenharia,
Universidade Federal do Paraná,
CEP 81531-990, Curitiba, PR, Brasil

[3]PPGMAE: Programa de Pós-graduação em Matemática Aplicada e Estatística,
Universidade Federal Rio Grande do Norte,
CEP 59087-900, Natal, RN, Brasil

[4]Department of Engineering, University of Durham, South Road,
Durham DH1 3LE, UK

corresponding author: carrer@ufpr.br

Summary

A Finite Element Method approach is presented for the solution of the two-dimensional wave-diffusion equation. The fractional time derivative is considered as a Caputo derivative. Houbolt and Newmark methods are employed for the time-marching process. Four examples are presented and discussed.

Introduction

It has, perhaps, become commonplace that many papers dealing with the solution of problems governed by differential equations with time and space derivatives of non-integer orders begin with or contain an excerpt from a famous letter written by Leibnitz to L'Hopital on 30 September 1695, in which some idea, or some reasoning, concerning fractional calculus is already present. By doing so, not only is the historical importance of the development of this important branch of mathematics highlighted, but tribute is also paid to the genius of one of the inventors of Differential Calculus. Returning to the mentioned letter excerpt: when inquired what if n were ½ in $\dfrac{d^n y}{dx^n}$, Leibnitz answered: "It will lead to a paradox, from which one day useful consequences will be drawn." Today, the many applications of fractional calculus found in science and in engineering confirm the Leibnitz' prediction and justify the growing attention that has been given to this branch of mathematics, see for instance Sun et al. [1], and Machado et al. [2], for an overview of the applications. Clear and didactic introductions to this matter are found in the works Fractional Calculus I, II, III, by Beardon [3], and the report by Loverro [4]. According to Miller and Ross [5]: "the name *fractional calculus* became somewhat of a misnomer. A better description might be *differentiation and integration to an arbitrary order*", as the theory of generalized operators had been extended to include operators of rational or irrational, positive or negative, real or complex orders. However, due to the tradition the name fractional calculus is kept in several textbooks, e.g., Oldham and Spanier [6], Ortigueira [7], Mainardi [8]. The great development of this research area must be credited to the development of the numerical methods which, by their turn, turned possible only with the advent of the digital computer. For formulations based on the Finite Difference Method (FDM), see for instance Murillo and Yuste [9], Yang et al. [10], Huang et al. [11]. Regarding formulations based on the Finite Element Method (FEM), the interested reader is referred to the works by Deng [12], Huang et al. [13], Zheng et al. [14], Corrêa et al. [15]. In what concerns the Boundary Element Method (BEM), see Katsikadelis [16], Dehghan and Safarpoor [17], Carrer at al. [18,19]. Meshless formulations have also been employed, see for instance Kumar et al. [20], Shekari et al. [21] and Zafarghandi et al. [22].

This work is concerned with the solution of the two-dimensional wave-diffusion equation through a Finite Element Method formulation. The Caputo integro-differential operator is adopted to represent the fractional time derivative, see [3,4]. The choice of the Caputo operator was influenced by the authors' previous successful experience in dealing with the solution of the same problem with the Boundary Element Method (BEM) formulation, see Carrer et al [18,19]. To represent the second order time derivative that appears in the Caputo operator, two approximations were adopted: the first is that due to Houbolt [23], and known as Houbolt method and, if widely used in BEM formulations, see [19], it is not used in FEM formulations, as it is prone to produce damping and period elongation in elasticity problems, see Bathe [24]; the second approximation is the Newmark method, widely used in FEM formulations, see [24,25,26]. The FEM formulation related to the former approximation will be called, from now on, FEM-WDH, and the designation FEM-WDN remains valid for the later approximation. To verify the potentialities of the proposed version of the FEM formulations, four examples are included and analysed. Different values of the order of the time derivative, which is usually represented by the Greek letter α, were adopted in each example. These values are: $\alpha = 2.0$, that corresponds to the classical wave propagation problem, and $\alpha = 1.8$, 1.5, 1.2, and 1.05. The comparison between the FEM results with the analytical solutions shows good agreement between them for the biggest values of α but, as α diminishes, FEM-WDN results loose accuracy while the FEM-WDH results continue keeping good accuracy. A comprehensive discussion is carried out in the section Examples.

2. The Wave-Diffusion Equation

The two-dimension wave-diffusion equation reads:

$$\frac{1}{c^2}\frac{\partial_C^\alpha u}{\partial t^\alpha} = \nabla^2 u \tag{1}$$

In Equation (1), ∇ is the Laplacian, c is the wave velocity, and $u = u(x,y,t)$ is a function of the space-time variables x,y,t. If $X = (x,y)$, a shortened notation arises and one can write: $u = u(X,t)$.

The fractional derivative $\frac{\partial_C^\alpha u}{\partial t^\alpha}$, $1 < \alpha < 2$, on the left-hand side of Equation (1), according to the Caputo definition is written as:

$$\frac{\partial_C^\alpha u}{\partial t^\alpha} = \frac{1}{\Gamma(2-\alpha)}\int_0^t \frac{1}{(t-\tau)^{\alpha-1}}\frac{\partial^2 u}{\partial \tau^2} d\tau \tag{2}$$

In Equation (2), Γ(…) is the Gamma function.

For a domain Ω, with the boundary Γ represented as: $\Gamma = \Gamma_u \cup \Gamma_q$, the boundary conditions are schematically defined as follows:

$$\text{Dirichlet boundary condition: } u(X,t) = \hat{u}(X,t), \text{ over } \Gamma_u \tag{3}$$

and

$$\text{Neumann boundary condition: } q(X,t) = \frac{\partial u}{\partial n} = \hat{q}(X,t) \text{ over } \Gamma_q \tag{4}$$

The initial conditions are:

$$u(X,0) = u_0(X) \tag{5}$$

$$\left.\frac{\partial u(X,t)}{\partial t}\right|_{t=0} = \dot{u}_0(X) \tag{6}$$

3. The Finite Element Method Formulation

The starting point for the development of the FEM formulations falls on the Galerkin method, Zienkiewicz and Taylor [27]. Here, the classical wave equation, for which $\alpha = 2$, is considered a particular case of a more general equation, which is precisely the fractional wave-diffusion equation.

The FEM equation that corresponds to Equation (1) is written as:

$$\boldsymbol{M}\frac{\partial_C^{\alpha}\boldsymbol{u}}{\partial t^{\alpha}} + \boldsymbol{K}\boldsymbol{u} = \boldsymbol{f} \tag{7}$$

In the above equation, $\boldsymbol{K}$ is the stiffness matrix:

$$\boldsymbol{K} = \int_{\Omega} \boldsymbol{B}^T \boldsymbol{B} d\Omega \tag{8}$$

$\boldsymbol{M}$ is the mass matrix:

$$\boldsymbol{M} = \int_{\Omega} \boldsymbol{N}^T \boldsymbol{N} d\Omega \tag{9}$$

and $\boldsymbol{f}$ is the load vector.

$$\boldsymbol{f} = \int_{\Gamma} \boldsymbol{N}^T q d\Gamma \tag{10}$$

Representing the interpolation, or shape, functions by N_1, N_2,…,N_n, one has:

$$\boldsymbol{B} = \begin{bmatrix} \frac{\partial N_1}{\partial x} & \frac{\partial N_2}{\partial x} & \cdots & \frac{\partial N_n}{\partial x} \\ \frac{\partial N_1}{\partial y} & \frac{\partial N_2}{\partial y} & \cdots & \frac{\partial N_n}{\partial y} \end{bmatrix} \tag{11}$$

$$\boldsymbol{N} = \begin{bmatrix} N_1 & N_2 & \dots & N_n \end{bmatrix} \tag{12}$$

To obtain the solution of Equation (1) at discrete time values, through Equation (7), requires the replacement of the second order time derivative, $\frac{\partial^2 u}{\partial \tau^2}$, in Equation (2), by an approximated formula. Among the many approximations found in the literature, two were adopted in this work, namely the Houbolt method [23], and the Newmark method [28]. For both approximations the solution is provided at the discrete times t_{n+1}. If Δt is the selected time interval, then $t_{n+1} = (n+1)\Delta t,\ 0 \le n \le N$, with N being defined by the researcher.

From now on, in order to simplify the notation, $\boldsymbol{u}(X,t_j)$, for any time t_j, is rewritten as $\boldsymbol{u}_j$. Equations (7), then, is suitably rewritten as:

$$\boldsymbol{M}\frac{\partial_C^\alpha \boldsymbol{u}_{n+1}}{\partial t^\alpha} + \boldsymbol{K}\boldsymbol{u}_{n+1} = \boldsymbol{f}_{n+1} \tag{13}$$

with:

$$\begin{aligned}&\frac{\partial_C^\alpha \boldsymbol{u}_{n+1}}{\partial t^\alpha} = \frac{1}{\Gamma(2-\alpha)}\int_0^{t_{n+1}} \frac{1}{(t-\tau)^{\alpha-1}}\frac{\partial^2 \boldsymbol{u}}{\partial \tau^2}d\tau = \\ &= \frac{1}{\Gamma(2-\alpha)}\left[\int_0^{t_1}\frac{1}{(t-\tau)^{\alpha-1}}\ddot{\boldsymbol{u}}_1 d\tau + \int_{t_1}^{t_2}\frac{1}{(t-\tau)^{\alpha-1}}\ddot{\boldsymbol{u}}_2 d\tau + \ldots + \int_{t_n}^{t_{n+1}}\frac{1}{(t-\tau)^{\alpha-1}}\ddot{\boldsymbol{u}}_{n+1} d\tau\right]\end{aligned} \tag{14}$$

The formulation based on the Houbolt method is called FEM-WDH: *FEM* for the Finite Element Method, WD for wave-diffusion equation, and H for the Houbolt method. In the Houbolt method a cubic Lagrange interpolation, from time $t_{j-2} = (j-2)\Delta t$ to time $t_{n+1} = (j+1)\Delta t$, is assumed for $\boldsymbol{u}$, and the second order derivative taken at $t = t_{j+1}$, thus generation what will be called the Houbolt approximation:

$$\left.\frac{\partial^2 \boldsymbol{u}}{\partial \tau^2}\right|_{t=t_{j+1}} = \ddot{\boldsymbol{u}}_{j+1} = \frac{\left(2\boldsymbol{u}_{j+1} - 5\boldsymbol{u}_j + 4\boldsymbol{u}_{j-1} - \boldsymbol{u}_{j-2}\right)}{\Delta t^2} \tag{15}$$

Equation (15) is substituted into Equation (14), and the following expression arises:

$$\frac{\partial_C^\alpha \boldsymbol{u}_{n+1}}{\partial\tau^\alpha} = \frac{1}{\Gamma(3-\alpha)\Delta t^\alpha}\Big\{\left(2\boldsymbol{u}_{n+1} - 5\boldsymbol{u}_n + 4\boldsymbol{u}_{n-1} - \boldsymbol{u}_{n-2}\right) +$$

$$\sum_{j=0}^{n-1}\left[\left(n+1-j\right)^{2-\alpha} - \left(n-j\right)^{2-\alpha}\right]\left(2\boldsymbol{u}_{j+1} - 5\boldsymbol{u}_j + 4\boldsymbol{u}_{j-1} - \boldsymbol{u}_{j-2}\right)\Big\} \quad (16)$$

Finally, the FEM-WDH corresponding equation is obtained after substituting Equation (16) into Equation (13). It can be written as:

$$\bar{\boldsymbol{K}}\boldsymbol{u}_{n+1} = \bar{\boldsymbol{f}}_{n+1} \quad (17)$$

in which:

$$\bar{\boldsymbol{K}} = \boldsymbol{K} + \frac{2}{\Gamma(3-\alpha)\Delta t^\alpha}\boldsymbol{M} \quad (18)$$

and

$$\bar{\boldsymbol{f}}_{n+1} = \boldsymbol{f}_{n+1} - \boldsymbol{M}\frac{1}{\Gamma(3-\alpha)\Delta t^\alpha}\Big[\left(-5\boldsymbol{u}_n + 4\boldsymbol{u}_{n-1} - \boldsymbol{u}_{n-2}\right) +$$

$$\sum_{j=0}^{n-1} B_{(n+1)j}\left(2\boldsymbol{u}_{j+1} - 5\boldsymbol{u}_j + 4\boldsymbol{u}_{j-1} - \boldsymbol{u}_{j-2}\right)\Big] \quad (19)$$

where:

$$B_{(n+1)j} = \left(n+1-j\right)^{2-\alpha} - \left(n-j\right)^{2-\alpha} \quad (20)$$

Note that the computation of $\boldsymbol{u}_{-2}$ and $\boldsymbol{u}_{-1}$ is required when $j=0$ is Equation (16), or in Equation (19). According to Carrer et al. [28], this can be done by employing the following expressions, see Carrer et al. [29]:

$$\boldsymbol{u}_{-2} = \boldsymbol{u}_0 - 2\Delta t\dot{\boldsymbol{u}}_0$$

$$\boldsymbol{u}_{-1} = \boldsymbol{u}_0 - \Delta t\dot{\boldsymbol{u}}_0 \quad (21)$$

The formulation based on the Newmark method [24], Newmark family of methods [25], or Newmark-β Method [26], is called FEM-WDN. Regarding the notation, the same reasoning can be followed, and N is used for Newmark. For the Newmark method, the following expressions for are used:

$$\left.\frac{\partial^2 \boldsymbol{u}}{\partial \tau^2}\right|_{t=t_{n+1}} = \ddot{\boldsymbol{u}}_{n+1} = \frac{\boldsymbol{u}_{n+1}}{\beta \Delta t^2} - \frac{\boldsymbol{u}_n}{\beta \Delta t^2} - \frac{\dot{\boldsymbol{u}}_n}{\beta \Delta t} - \left(\frac{1}{2\beta} - 1\right)\ddot{\boldsymbol{u}}_n \tag{22}$$

$$\left.\frac{\partial \boldsymbol{u}}{\partial \tau}\right|_{t=t_{n+1}} = \dot{\boldsymbol{u}}_{n+1} = \dot{\boldsymbol{u}}_n + \Delta t\left(1-\delta\right)\ddot{\boldsymbol{u}}_n + \delta \Delta t \ddot{\boldsymbol{u}}_{n+1} \tag{23}$$

The corresponding version for Equation (17) has:

$$\bar{\boldsymbol{K}} = \boldsymbol{K} + \frac{1}{\Gamma(3-\alpha)\beta \Delta t^{\alpha}} \boldsymbol{M} \tag{24}$$

$$\bar{\boldsymbol{f}}_{n+1} = \boldsymbol{f}_{n+1} + \frac{1}{\Gamma(3-\alpha)} \boldsymbol{M} \left\{ \frac{\boldsymbol{u}_n}{\beta \Delta t^{\alpha}} + \frac{\dot{\boldsymbol{u}}_n}{\beta \Delta t^{\alpha-1}} + \left(\frac{1}{2\beta} - 1\right) \frac{\ddot{\boldsymbol{u}}_n}{\beta \Delta t^{\alpha-2}} + \right.$$
$$\left. \sum_{j=0}^{n-1} B_{(n+1)j} \left[\frac{\boldsymbol{u}_{j+1}}{\beta \Delta t^{\alpha}} - \frac{\boldsymbol{u}_j}{\beta \Delta t^{\alpha}} - \frac{\dot{\boldsymbol{u}}_j}{\beta \Delta t^{\alpha-1}} - \left(\frac{1}{2\beta} - 1\right) \frac{\ddot{\boldsymbol{u}}_j}{\beta \Delta t^{\alpha-2}} \right] \right\} \tag{25}$$

The term $\ddot{\boldsymbol{u}}_0$, that appears in Equation (25) when $j = 0$, is computed directly from differential equation related to the classical wave propagation problem.

The presence of the summation symbol in Equations (19) and (25) means that the computation of the variable of interest, $\boldsymbol{u}$, at time t_{n+1}, involves all its previous values. In other words, the computation depends on the history. This is a consequence of the non-local character of the Caputo operator.

4. Examples

Once the FEM-WDH and FEM-WDN basic equations have been obtained, four examples were analysed to verify the pros and cons of each one of them. Starting with $\alpha = 2.0$, that corresponds to the classical wave propagation problem, the other values of the fractional order of the time derivative adopted are: $\alpha = 1.8, 1.5, 1.2, 1.05$.

The adoption of small values for α such as $\alpha = 1.2$ or $\alpha = 1.05$ poses a challenge. In authors' previous works that deal with BEM formulations, accurate results for small values of α, such as $\alpha = 1.2$ or $\alpha = 1\ 05$, only were obtained with a Caputo derivative-based formulation, see Carrer et al. [19]; in their formulation based on the Riemann-Liouville derivative, see Carrer et al. [30], accurate results were obtained only for $\alpha > 1.5$, demonstrating a severe limitation of that formulation. It seems that Caputo-derivative based formulations are the only ones capable to provide accurate results for small values of α. Additionally, in a FEM Caputo derivative-based formulation for the anomalous diffusion problem, see Corrêa et al. [15], accurate results could be found for values of α as small as $\alpha = 0.05$. The above comments justify the authors' choice for the development of the FEM-WDH and FEM-WDN formulations.

Regarding the FEM-WDH formulation, perhaps the use of the Houbolt method can bring some surprise for some readers, mainly to those that got used with the use of the Newmark method. However, despite the comments by Cook et al. [25]: "The Houbolt method was once common in general-purpose transient codes but has been supplanted by methods with better algorithmic damping properties and now is more of historical interest.", the FEM-WDN results are always in better agreement with the analytical solutions than the FEM-WDN results. In fact, in all the examples included here the FEM-WDN formulations fails in providing accurate results for the smaller values of the order of the time derivative, see Figures 20 – 21 and 35 – 36.

The selection of the time-step length is based on the authors' previous experience with the BEM formulations based on the use of the Houbolt method, see Carrer et al. [30]. The use of the Newmark method for problems belonging to the fractional calculus constitutes a novelty that deserves be mentioned. As is widely known, the Newmark method is unconditionally stable for $\beta = 0.25$ and $\delta = 0.50$;keeping these values, the same time-step could be adopted for both formulations. Note that various attempts to use alternative values for β and δ, whose results are not included here, were unsuccessful even with the adoption of much smaller time-steps. The presence of, say, a kind of damping that appears when $\alpha < 2.0$, enables the use of the time step adopted for the classical problem and allow the authors to postpone the development of a stability analysis study. In fact, this is still a challenging task.

In all the examples, $c = 1.0$. The meshes are characterized by the number of elements, n_{Ω}, and the by the number of degrees of freedom or, concisely, the number of nodes, by n_{nodes}.

4.1. Bar with sinusoidal initial condition

This example consists of a bar of length $L = \pi$, fixed at $x = 0$ and $x = \pi$, see Figure 1, with the initial conditions:

$$u_0(x) = \sin x \tag{26}$$

$$\dot{u}_0(x) = 0 \tag{27}$$

From the depiction of the problem, as well as from Equations (26) and (27), it is readily seen that this is a one-dimensional problem. To solve it using the formulations developed here, a rectangular domain defined in the region $0 \le x \le \pi$, $0 \le y \le \pi/2$ replaces the original domain for the two-dimensional FEM analyses. The boundary conditions for this rectangular domain are written as:

$$u(0, y, t) = 0\,;\; u(\pi, y, t) = 0 \tag{28}$$

$$q(x, 0, t) = \left.\frac{du}{dn}\right|_{(x,0,t)} = 0\,;\; q(x, \pi/2, t) = \left.\frac{du}{dn}\right|_{(x,\pi/2,t)} = 0 \tag{29}$$

Note that the simulation of the one-dimensional is accomplished through the Neumann boundary conditions, see Equation (29), at $y = 0$ and $y = \pi/2$.

The mesh is depicted in Figure 2 and has $n_\Omega = 128$, and $n_{nodes} = 153$. The time-step is $\Delta t = 0.025$. The FEM results are compared with the analytical solution, see Murillo and Yuste [9]:

$$u(x,t) = E_\alpha\left(-t^\alpha\right)\sin x \tag{30}$$

where $E_\alpha(\ldots)$ is the Mittag-Leffler function, see Miller and Ross [5], Ortigueira [7], omnipresent in the analytical solutions of the next examples. It is defined as:

$$E_\alpha(z) = \sum_{k=0}^{\infty} \frac{z^k}{\Gamma(1+\alpha k)} \tag{31}$$

where $z \in C$, α is the fractional order of the derivative, and $\Gamma(\ldots)$ is the gamma function. For $\alpha = 2$ one has:

$$E_2\left(-z^2\right) = \cos z \tag{32}$$

This is a very simple problem, for which the function $E_\alpha(-t^\alpha)$ is easily evaluated and has been employed by many authors for verifying the accuracy of numerical methods, see for instance Murillo and Yuste [9], Carrer et al. [19]. The results from FEM-WDH and FEM-WDN formulations, here and in the following examples, will be displayed side-by-side whenever possible. The results for $u(\pi/2,\pi/4,t)$ are depicted in Figure 3; and the results for $u(x,\pi/4,3)$ is shown in Figure 4. Note that even for small values of α, a good agreement between the FEM results and the analytical solution is observed. Besides, from Figure 3 one can notice that a kind of damping appears as α becomes smaller and the vibrational movement practically comes to an end.

4.2. Bar with Neumann boundary condition

This example consists of a bar of length $L = 12$, fixed at $x = 0$, and subjected to a Neumann boundary condition, that can be interpreted as a suddenly applied load, at $x = L$, see Figure 5. The boundary conditions for this one-dimensional problem are:

$$u(0,t) = 0 \tag{33}$$

$$q(L,t) = \bar{q}\, H(t-0) \tag{34}$$

Regarding Equation (34):

$$\bar{q} = \frac{\partial u}{\partial x} = \varepsilon = \frac{P}{EA} \tag{35}$$

where the deformation, ε, is a function of the longitudinal elasticity modulus, E, of the area of the transversal section A, and of the applied load, P.

The problem also presents null initial conditions.

The boundary conditions in Equations (33) and (34) enable one to rephrase the description of this problem as representing the longitudinal vibration of a bar subjected to a load suddenly applied and kept constant during all the time of analysis. When $\alpha = 2$ this problem is characterized by the presence of jumps in the results for $q(0,t)$, that is, the results for $q(0,t)$ present discontinuities in time. Due to the difficulty of numerical methods in correctly displaying, or rather, in depicting these discontinuities, the results for $q(0,t)$ can be used to assess the capability of the proposed numerical method to provide accurate solutions to the problem.

The analytical solution is, see Carrer et al. [30]:

$$u(x,t) = \bar{q}\left(x - \frac{8L}{\pi^2} \sum_{n=1,3,5,\dots}^{\infty} \frac{1}{n^2} \sin\left(\frac{n\pi}{2}\right) E_\alpha\left(-\lambda_n^2 c^2 t^\alpha\right) \sin(\lambda_n x) \right) \tag{36}$$

with:

$$\lambda_n = \frac{n\pi}{2L} \tag{37}$$

As before, the solution of this problem was sought through the definition of an equivalent problem in the rectangular domain, $0 \le x \le L$, $0 \le y \le L/2$, that presents null Neumann boundary conditions at $y = 0$ and $y = L/2$ in order to simulate the original one-dimensional problem. In this way, the boundary conditions of the equivalent problem are:

$$u(0, y, t) = 0\,; q(L, y, t) = \bar{q} \tag{38}$$

$$q(x, 0, t) = \left.\frac{du}{dn}\right|_{(x,0,t)} = 0\,;\; q(x, L/2, t) = \left.\frac{du}{dn}\right|_{(x,L/2,t)} = 0 \tag{39}$$

The mesh is that already employed in the first example, scaled to accommodate the different domain size.

Now, the time-step used in all analyses is $\Delta t = 0.25$.

The results for $u(L,L/4,\ t)$ and $u(L/2,L/4,\ t)$ are depicted in Figures 6 to 8. Regarding those figures, there are some important observations: *i*) the oscillatory motion for u in Figure 6 tends to disappear, see Figures 7 and 8, and is practically absent for $\alpha = 1.05$; *ii*) the FEM-WDN results present an increasing loss of accuracy, mainly for $\alpha = 1.05$, see Figure 8.

The results for $q(0,\ L/4,\ t)$ and are depicted in Figures 8 to 11. Note that the time jumps presented by q at $x = 0$, see Figure 9, tend to disappear as α becomes smaller than 2, see Figures 10 and 11. As expected after the results for u, the FEM-WDN results lose accuracy for $\alpha = 1.05$, see Figure 11. But which really draws the attention appears in Figure 9: while the FEM-WDH results present a reasonable agreement with the analytical solution, with the discontinuities being well represented, on the other hand the FEM-WDN results fail in correctly representing the jumps since the beginning of the analysis. The damping introduced by the Houbolt method is benefic for this kind of problem. The same can be said about the use of the Houbolt method in BEM formulations, see, for instance, Carrer et al. [19].

Figure 12 present the results for $u(x,L/2,18)$.

As an overall conclusion, from the classical wave propagation problem to the problems presenting small values of α and presented here, FEM-WDH results are in good agreement with the analytical solution; the FEM-WDN results are acceptable only for $\alpha = 1.5$.

4.3. Square Domain with Sinusoidal Initial Condition

The problem to be solved in this third example, illustrated in Figure 13, is defined in the region $0 \le x,y \le L$, with $L = 10$, and presents the boundary conditions:

$$u(x,y,t)=0 \text{ for } x=0 \text{ and } x=L \tag{33}$$

$$u(x,y,t)=0 \text{ for } y=0 \text{ and } y=L \tag{34}$$

The initial conditions are:

$$u_0(x,y)=U\sin\left(\frac{\pi x}{L}\right)\sin\left(\frac{\pi y}{L}\right) \tag{35}$$

$$\dot{u}_0(x,y)=0 \tag{36}$$

For the analytical solution, one has, see Carrer et al. [30]:

$$u(x,y,t)=E_\alpha\left(-\frac{2\pi^2}{L^2}c^2t^\alpha\right)\sin\left(\frac{\pi x}{L}\right)\sin\left(\frac{\pi y}{L}\right) \tag{37}$$

The above expression, when particularized for $\alpha = 2.0$, is written as:

$$u(x,y,t)=\cos\left(\frac{\sqrt{2}\pi}{L}ct\right)\sin\left(\frac{\pi x}{L}\right)\sin\left(\frac{\pi y}{L}\right) \tag{38}$$

To verify the accuracy and the convergence of the FEM-WDH and FEM-WDN results to the analytical solution, the relative L^2 error norm, E_2, was computed according to:

$$E_2=\frac{\left\|u_{analytical}-u_{FEM}\right\|_{L^2(\Omega)}}{\left\|u_{analytical}\right\|_{L^2(\Omega)}}=\frac{\sqrt{\iint_\Omega\left(u_{analytical}-u_{FEM}\right)^2 d\Omega}}{\sqrt{\iint_\Omega\left(u_{analytical}\right)^2 d\Omega}}\cong\frac{\sqrt{\sum_{i=1}^{N}\left(u^i_{analytical}-u^i_{FEM}\right)^2}}{\sqrt{\sum_{i=1}^{N}\left(u^i_{analytical}\right)^2}} \tag{39}$$

In Equation (39) u_{FEM} represents either the FEM-WDH or the FEM-WDN results, obtained with the use of three regular meshes with increasing level of discretzation. In the first mesh, $n_\Omega = 100$, and $n_{nodes} = 121$. For this mesh, the analyses were carried out with $\Delta t = 0.15$. The second mesh has $n_\Omega = 400$ and $n_{nodes} = 441$. For this mesh, $\Delta t = 0.075$. For the third and more refined mesh, $n_\Omega = 1600$ and $n_{nodes} = 1681$, see Figure 14. The corresponding time-step is $\Delta t = 0.0375$.

The results related to E_2 are shown first; see Figures 15 and 16 for the times $t = 3.0$ and $t = 6.0$, respectively.

Aiming at providing the reader a more comprehensive discussion, BEM results were also included in the above-mentioned figures. It is important to mention that each one of the three BEM analyses was carried out with the same time-step and the same data regarding n_{nodes} of the corresponding FEM analyses. The authors would like to emphasize that the BEM formulation, such as that presented by Carrer at al. [30], employs linear triangular cells in the domain discretization; for this example, 200 cells were employed in the first analysis, 800 in the second and 3200 in the third and last one.

From Figures 15 and 16, one can notice that for $\alpha = 2.0$ the FEM-DWN performs better than the FEM-DWH, but this is an exception: at $t = 3.0$, FEM-DWN produces results in better agreement with the analytical solution for $\alpha = 1.8$ and $\alpha = 1.5$, whereas for $\alpha = 1.2$ and $\alpha = 1.05$ this statement is valid for the FEM-DWH results. On the other hand, at $t = 6.0$, the FEM-DWH results, for $\alpha \neq 2.0$, are in better agreement with the analytical solution than the FEM-DWN ones. The best BEM results, for both times, are those obtained for $\alpha = 1.2$ and $\alpha = 1.05$.

The results for $u(L/2,L/2,t)$ are depicted in Figure 17, where a good agreement is observed between the FEM-DWH and FEM-DWN results and the analytical solution for all values of α. The results in Figure 17 follow the same pattern of those previously presented in Figure 3, that is, the decreasing in α is accompanied by the ceasing of the oscillatory behaviour: for $\alpha = 2.0$, one has a periodic and undamped response; for $\alpha = 1.8$, the oscillatory behaviour still continues but the presence of damping is to be noted; for $\alpha = 1.5$ a little oscillation can be noticed, but the damping is greater than that for $\alpha = 1.8$. The results for $\alpha = 1.2$ and $\alpha = 1.05$ present no oscillation.

FEM-WDH and FEM-WDN results for $u(x,L/2,3)$ in Figure 18 present good agreement with the analytical solution for the three meshes.

4.4. Circular domain with a linear initial condition

This last example consists of a circular domain and, therefore, it is better described by a polar coordinate system (r,θ), $0 \le r \le R = 10$, $0 \le \theta \le 2\pi$, see Figure 19. In this system of coordinates, one has the boundary condition given by:

$$u(R,t) = 0 \tag{40}$$

For the initial conditions, one has:

$$u_0(r) = 1 - \frac{r}{R} \tag{41}$$

$$\dot{u}_0(r) = 0 \tag{42}$$

The variables are independent from the coordinate θ and the analytical solution reads, see Carrer et al. [30]:

$$u(r,t) = \sum_{n=1}^{\infty} J_0\left(z_n \frac{r}{R} \right) H_n E_\alpha(\omega_n^2 t^\alpha) \tag{43}$$

In Equation (43), z_n are the zeros of the Bessel function of the first kind and order zero, obtained from:

$$J_0(z_n) = 0 \tag{44}$$

Besides:

$$\omega_n = \frac{z_n c}{R} \tag{45}$$

and:

$$H_n = \frac{2}{R^2\left[J_1(z_n)\right]^2}\int_0^R u_0(r)J_0\left(z_n\frac{r}{R}\right)rdr \tag{46}$$

The substitution of Equation (41) into Equation (46) gives:

$$H_n = \frac{2}{R^2\left[J_1(z_n)\right]^2}\left[\frac{R^2}{z_n}J_1(z_n) - \frac{R^2}{3}\,{}_1F_2\left(\frac{3}{2};\ 1,\frac{5}{2};-\frac{z_n^2}{4}\right)\right] \tag{46}$$

The generalized hypergeometric function, ${}_1F_2(\ldots)$, in Equation (46), is computed as:

$${}_1F_2\left(\frac{3}{2};1,\frac{5}{2};-z\right) = \frac{3}{8z}\left[J_1\left(2\sqrt{z}\right)\left(4\sqrt{z} - \pi H_0\left(2\sqrt{z}\right)\right) + \pi J_0\left(2\sqrt{z}\right)H_1\left(2\sqrt{z}\right)\right] \tag{47}$$

In Equation (47) $J_1(\ldots)$ is the Bessel function of the first kind and order one, and $H_0(\ldots)$ and $H_1(\ldots)$ are the Struve functions of orders zero and one, respectively. When $\alpha = 2.0$, one retrieves the expression given by Greenberg [31] for the classical wave propagation problem:

$$u(r,t) = \sum_{n=1}^{\infty} J_0\left(z_n\frac{r}{R}\right)H_n\cos(\omega_n t) \tag{48}$$

In order to have a better representation of problem geometry, six-nodes triangular elements meshes were adopted. These meshes are depicted in Figures 20 – 22, and are called: mesh 1, with $n_\Omega = 144$, $n_{nodes} = 305$; mesh 2, with $n_\Omega = 576$, $n_{nodes} = 1185$; mesh 3, with $n_\Omega = 2394$, $n_{nodes} = 4673$. The corresponding time steps are: Δt = 0.8, for mesh 1, Δt = 0.4, for mesh 2, and Δt = 0.2, for mesh 3.

FEM-WDH and FEM-WDN results, obtained with mesh 3, for $u(0,t)$, $u(2,t)$, $u(4,t)$, $u(6,t)$, and $u(8,t)$ are shown in Figures 23 – 25. FEM-WDH results are always in good agreement with the analytical solution. The FEM-WDN results, on the other hand, can be considered good for $\alpha = 2.0$ and acceptable only for $\alpha = 1.5$. For the smaller values of α, that is, for $\alpha = 1.05$ the FEM-WDN results present a strong disagreement with the analytical solution, thus suggesting the use of more refined meshes or, which seems to be more reasonable, the use of different values for the parameters β and δ. One can arrive at the same conclusion from Figure 26, which display the results for $u(r,12)$.

Quite good results were produced by the FEM-WDH formulation while the results produced by the FEM-WDN formulation were quite disappointing. Regarding this last observation, it seems that the FEM-WDN formulation, or rather, the Newmark method, proved to be incapable of producing accurate results with the values commonly used for the β and δ parameters. Figures 27 and 28, that contain the convergence study for this example, only confirm this conclusion: there, it is readily seen that FEM-WDH performs much better than the FEM-WDN for all the chosen values of α.

Conclusion

Nowadays, fractional calculus problems are under the focus of intense research, both from the theoretical and from the numerical point of view. In this work, the authors intend to present a small contribution towards the solution of the diffusion-wave problems through formulations based on the Finite Element Method. Two formulations were developed with this aim and were called FEM-WDH and FEM-WDN; the former is based on the use of the Houbolt method and the later, on the use of the Newmark method to perform the time-marching process. Although, to the authors' knowledge, the Houbolt method is not currently being used in FEM formulations, its successful use in BEM formulations encouraged the development of the FEM-WDH formulation. The results presented in this work evidenced the appropriateness of this choice and also brought a certain disappointment in relation to the FEM-WDN formulation: while the FEM-WDH results are always in good agreement with the analytical solutions, the FEM-WDN formulation was unable to produce accurate results for small values of alpha in the second and, especially, the fourth example. It is thought that further research should be done regarding the choice of β and δ parameters when using Newmark's method for solving fractional calculus problems. Perhaps some conclusions found in textbooks should be rethought in the light of the results presented here and, perhaps, to be presented in the future by other researchers. Naturally much effort has still to be done regarding the solution of problems governed by fractional partial differential equations and, as mentioned at the beginning to this Conclusion, this work is intended to present a small contribution for those interested in numerical methods in general.

Acknowledgments

The authors respectfully acknowledge Coordenação de Aperfeiçoamento de Pessoal de Nível Superior – Brasil (CAPES) and Conselho Nacional de Desenvolvimento Científico e Tecnológico (CNPq) for the financial support.

References

[1] Sun H, Zhang Y, Baleanu D, Chen W, Chen Y. A new collection of real world applications of fractional calculus in science and engineering. Communications in Nonlinear Science and Numerical Simulation 2018; **64**, 213 – 231.

[2] Machado JAT, Silva MF, Barbosa RS, Jesus IS, Reis CM, Marcos MG, Galhano AF. Some Applications of Fractional Calculus in Engineering. *Mathematical Problems in Engineering*, 2010, Article ID 639801, 34 pages, doi:10.1155/2010/639801

[3] Beardon A. Fractional Calculus I, available at https://nrich.maths.org/1365; Fractional Calculus II, available at https://nrich.maths.org/1369; Fractional Calculus III, available at https://nrich.maths.org/1371, 2000.

[4] Loverro A. *Fractional Calculus: History, Definitions and Applications for the Engineer*. Department of Aerospace and Mechanical Engineering, University of Notre Dame, 2004

[5] Miller KS, Ross B. *An Introduction to the Fractional Calculus and Fractional Differential Equations*, John Wiley & Sons, 1993.

[6] Oldham KB, Spanier J. *The Fractional Calculus. Theory and Applications of Differentiation and Integration to Arbitrary Order*, Academic Press, Inc., 1974.

[7] Ortigueira MD. *Fractional Calculus for Scientists and Engineers*, Lecture Notes in Electrical Engineering, volume 84, 2011, Springer.

[8] Mainardi F. *Fractional Calculus: Theory and Applications*. Printed edition of the special issue published in *Mathematics*, MDPI, Basel, Switzerland, 2018.

[9] Murillo JQ, Yuste SB. An Explicit Difference Method for Solving Fractional Diffusion and Diffusion-Wave Equations in the Caputo Form, *Journal of Computational and Nonlinear Dynamics*, 2011; **6**, https://doi.org/10.1115/1.4002687

[10] Yang Q, Liu F, Turner I. Numerical methods for fractional partial differential equations with Riesz space fractional derivatives, *Applied Mathematical Modelling*, 2010; **34**, 200-218.

[11] Huang J, Tang Y, Vázquez L Yang J. Two finite difference schemes for time fractional diffusion-wave equation. *Numerical Algorithms,* 2013; **64**, 707–720. https://doi.org/10.1007/s11075-012-9689-0

[12] Deng WH. Finite Element Method for the Space and Time Fractional Fokker-Planck Equation, *SIAM Journal on Numerical Analysis*, 2008; **47**, 204-226.

[13] Huang Q, Huang G, Zhan H. A Finite Element Solution for the Fractional Advection-Dispersion Equation, *Advances in Water Resources*, 2008; **31**, 1578-1589.

[14] Zheng Y, Li C, Zhao Z. A note on the finite element method for the space fractional advection diffusion equation, *Computers and Mathematics with Applications*, 2010; **59**, 1718-1726.

[15] Corrêa RM, Carrer JAM, Solheid BS, Trevelyan J. The solution of the anomalous diffusion equation by a finite element method formulation based on the Caputo derivative, *Journal of the Brazilian Society of Mechanical Sciences and Engineering*, 2022; **44**, 250. https://doi.org/10.1007/s40430-022-03544-5

[16] Katsikadelis JT. The BEM for Numerical Solution of Partial Fractional Differential Equations, *Computers and Mathematics with Applications*, 2011; **62**, 891-901.

[17] Dehghan M, Safarpoor M. The Dual Reciprocity Boundary Elements Method for the Linear and Nonlinear Two-Dimensional Time-Fractional Partial Differential Equations, *Mathematical Methods in the Applied Sciences*, 2016, **39**, 3979-3995.

[18] Carrer JAM, Solheid BS, Trevelyan J, Seaid M. A boundary element method formulation based on the Caputo derivative for the solution of the anomalous diffusion problem, *Engineering Analysis with Boundary Elements*, 2021; **122**, 132-144.

[19] Carrer JAM, Solheid BS, Trevelyan J, Seaid M. A boundary element method formulation based on the Caputo derivative for the solution of the diffusion-wave equation. *Engineering with Computers*, 2022; **38**, 3563–3580. https://doi.org/10.1007/s00366-021-01480-x

[20] Kumar A, Bhardwaj A, Kumar BVR. A meshless local collocation method for time fractional diffusion wave equation. *Computers and Mathematics with Applications*, 2019; **78**, 1851-1861.

[21] Shekari Y, Tayebi A, Heydary MH. A meshfree approach for solving 2D variable-order fractional nonlinear diffusion-wave equation, *Computer Methods in Applied Mechanics and Engineering*, 2019; **350**, 154-168.

[22] Zafarghandi FS, Mohammadi M, Babolian E, Javadi S. Radial Basis Functions Method for Solving the Fractional Diffusion Equations, *Applied Mathematics and Computation*, 2019; **342**, 224-246.

[23] Houbolt JC. A Recurrence Matrix Solution for the Dynamic Response of Elastic Aircraft, *Journal of the Aeronautical Sciences*, 1950; **17**, 540-550.

[24] Bathe KJ. *Finite element procedures*. Prentice Hall, New Jersey, 1996.

[25] Cook RD, Malkus DS, Plesha ME. *Concepts and Applications of Finite Element Analysis*. John Wiley & Sons, Inc. 1989.

[26] Weaver, Jr W, Johnston PR. *Structural Dynamics by Finite Elements*. Prentice Hall, New Jersey, 1987.

[27] Zienkiewicz, OC and Taylor, RL. *The finite element method for solid and structural mechanics*. Elsevier Butterworth-Heinemann, 6th edition, 2005.

[28] Newmark NM. A Method of Computation for Structural Dynamics, ASCE, J. Eng. Mech. Div., 85, No. EM3, 1959, pp. 67 – 94.

[29] Carrer JAM, Mansur WJ, Vanzuit RJ. Scalar wave equation by the boundary element method: a D-BEM approach with non-homogeneous initial conditions, *Computational Mechanics*, 2009; **44**, 31-44.

[30] Carrer JAM, Solheid BS, Trevelyan J, Seaid M. The Boundary Element Method applied to the solution of the diffusion-wave problem, *Engineering Analysis with Boundary Elements*, 2020; **117**, 13–25.

[32] Greenberg MD. Advanced Engineering Mathematics, 1998, Prentice-Hall.

Caption to the figures

Figure 1. Bar with sinusoidal initial condition: geometry and boundary conditions for the two-dimensional simulation.

Figure 2. Mesh used in the first and second examples: $n_\Omega = 128$, $n_{nodes} = 153$.

Figure 3. Bar with sinusoidal initial condition: FEM-WDH and FEM-WDN results for $u(\pi/2,\pi/4,t)$.

Figure 4. Bar with sinusoidal initial condition: FEM-WDH and FEM-WDN results for $u(x,\pi/4,3)$.

Figure 5. Bar with suddenly applied load: geometry and boundary conditions for the two-dimensional simulation.

Figure 6. Bar with suddenly applied load: FEM-WDH and FEM-WDN results for $u(L,L/2,t)$ and $u(L/2,L/2,t)$ with $\alpha = 2.0$.

Figure 7. Bar with suddenly applied load: FEM-WDH and FEM-WDN results for $u(L,L/2,t)$ and $u(L/2,L/2,t)$ with $\alpha = 1.5$.

Figure 8. Bar with suddenly applied load: FEM-WDH and FEM-WDN results for $u(L,L/2,t)$ and $u(L/2,L/2,t)$ with $\alpha = 1.05$.

Figure 9. Bar with suddenly applied load: FEM-WDH and FEM-WDN results for $q(0,L/2,t)$ with $\alpha = 2.0$.

Figure 10. Bar with suddenly applied load: FEM-WDH and FEM-WDN results for $q(0,L/2,t)$ with $\alpha = 1.5$.

Figure 11. Bar with suddenly applied load: FEM-WDH and FEM-WDN results for $q(0,L/2,t)$ with $\alpha = 1.05$.

Figure 12. Bar with suddenly applied load: FEM-WDH and FEM-WDN results for $u(x,L/2,18)$.

Figure 13. Square domain: geometry and boundary conditions.

Figure 14. Square domain: mesh with $n_\Omega = 1600$, $n_{nodes} = 1681$.

Figure 15. Square domain: convergence study, for FEM and BEM analyses, at $t = 3.0$

Figure 16. Square domain: convergence study, for FEM and BEM analyses, at $t = 6.0$.

Figure 17 Square domain: FEM-WDH and FEM-WDN results $u(L/2,L/2,t)$.

Figure 18. Square domain: FEM-WDH and FEM-WDN results $u(x,L/2,3)$.

Figure 19. Circular domain: geometry and boundary conditions.

Figure 20. Circular domain: mesh 1 with $n_\Omega = 144$, $n_{nodes} = 305$.

Figure 21. Circular domain: mesh 2 with $n_\Omega = 576$, $n_{nodes} = 1185$.

Figure 22. Circular domain: mesh 3 with $n_\Omega = 2394$, $n_{nodes} = 4673$.

Figure 23. Circular domain: FEM-WDH and FEM-WDN results for $u(0,t)$, $u(2,t)$, $u(4,t)$, $u(6,t)$, and $u(8,t)$ with $\alpha = 2.0$.

Figure 24. Circular domain: FEM-WDH and FEM-WDN results for $u(0,t)$, $u(2,t)$, $u(4,t)$, $u(6,t)$, and $u(8,t)$ with $\alpha = 1.5$.

Figure 25. Circular domain: FEM-WDH and FEM-WDN results for $u(0,t)$, $u(2,t)$, $u(4,t)$, $u(6,t)$, and $u(8,t)$ with $\alpha = 1.05$.

Figure 26. Circular domain: FEM-WDH and FEM-WDN results for $u(r,12)$.

Figure 27. Circular domain: convergence study at $t = 12.0$.

Figure 28. Circular domain: convergence study at $t = 28.0$.

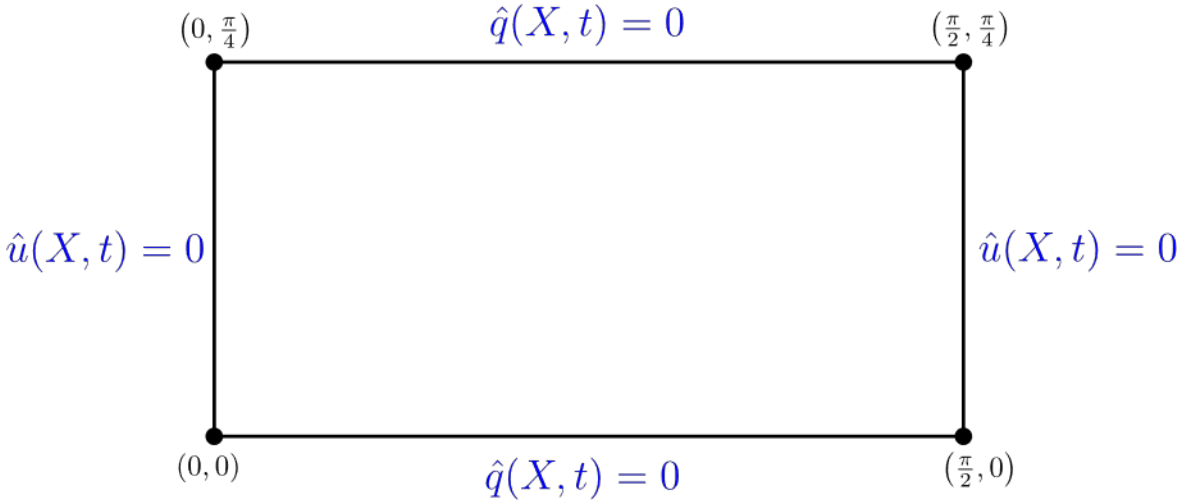
$(0, \frac{\pi}{4})$
$\hat{q}(X,t) = 0$
$(\frac{\pi}{2}, \frac{\pi}{4})$
$\hat{u}(X,t) = 0$
$\hat{u}(X,t) = 0$
$(0,0)$
$\hat{q}(X,t) = 0$
$(\frac{\pi}{2}, 0)$

FIGURE 1

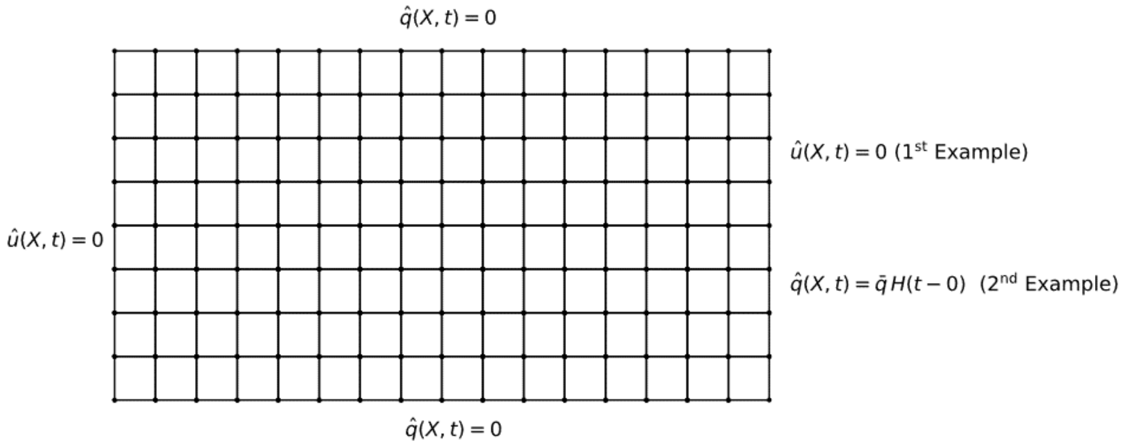
$\hat{q}(X,t)=0$
$\hat{u}(X,t)=0$ (1st Example)
$\hat{u}(X,t)=0$
$\hat{q}(X,t)=\bar{q}\,H(t-0)$ (2nd Example)
$\hat{q}(X,t)=0$

FIGURE 2

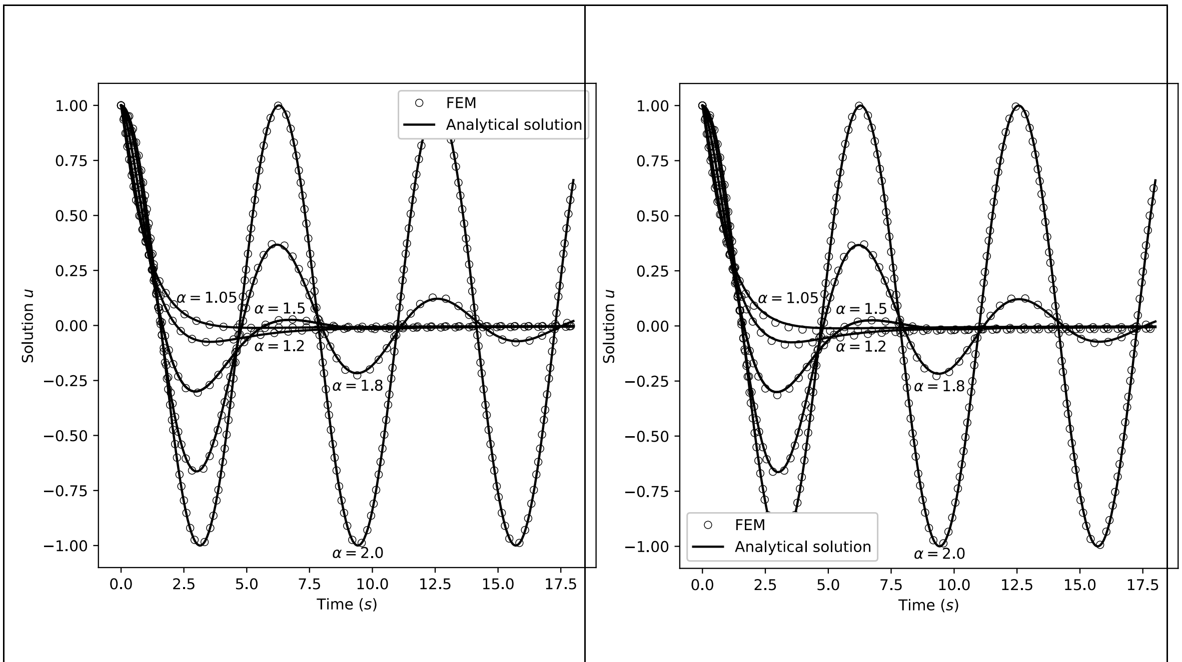

(a) FEM-WDH

(b) FEM-WDN

FIGURE 3

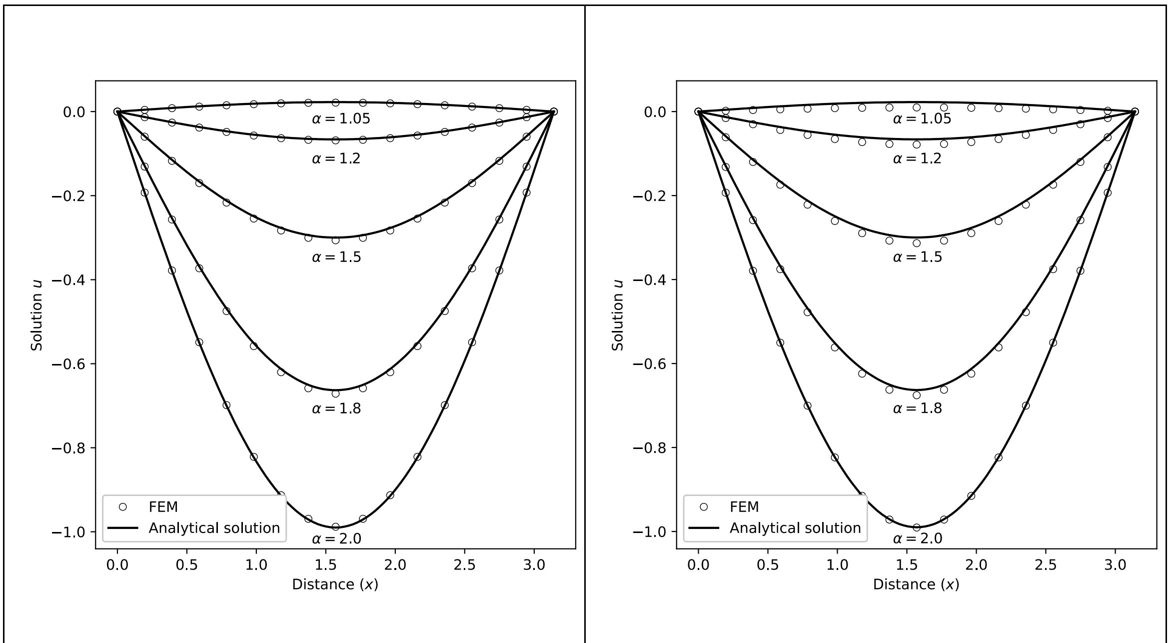

(a) FEM-WDH

(b) FEM-WDN

FIGURE 4

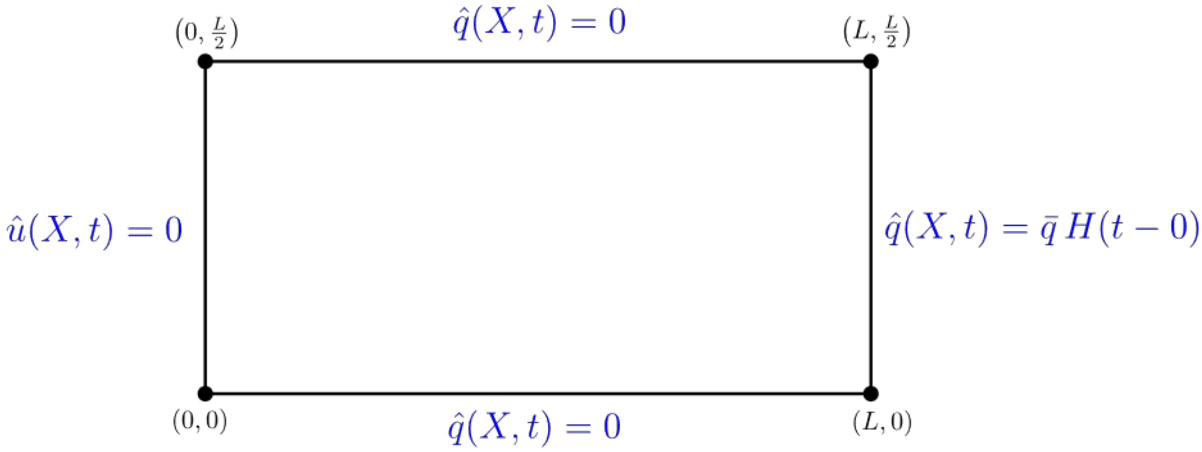
$\hat{q}(X,t)=0$
$(0,\frac{L}{2})$
$(L,\frac{L}{2})$
$\hat{u}(X,t)=0$
$\hat{q}(X,t)=\bar{q}\,H(t-0)$
$(0,0)$
$(L,0)$
$\hat{q}(X,t)=0$

FIGURE 5

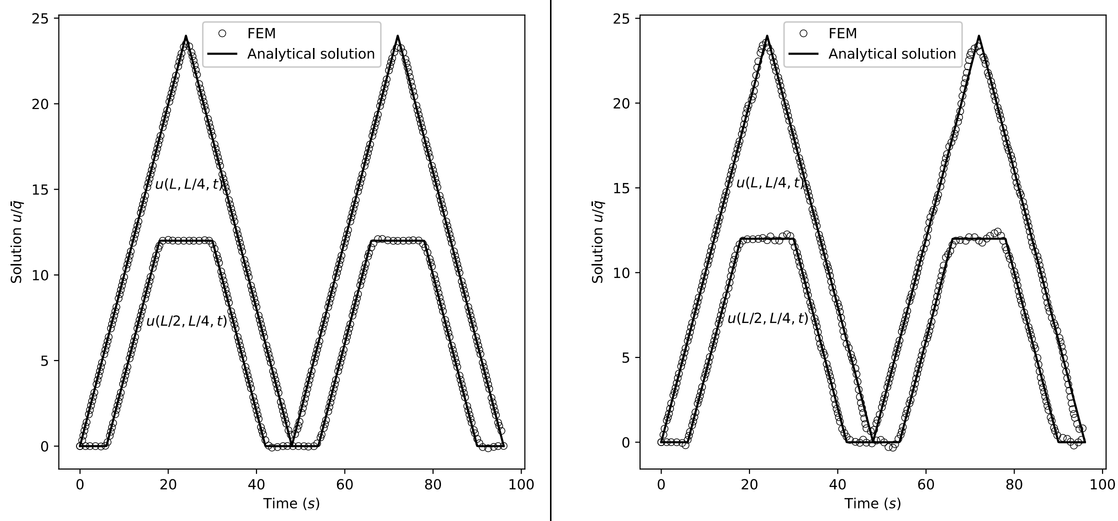

(a) FEM-WDH (α = 2.0)

(b) FEM-WDN (α = 2.0)

FIGURE 6

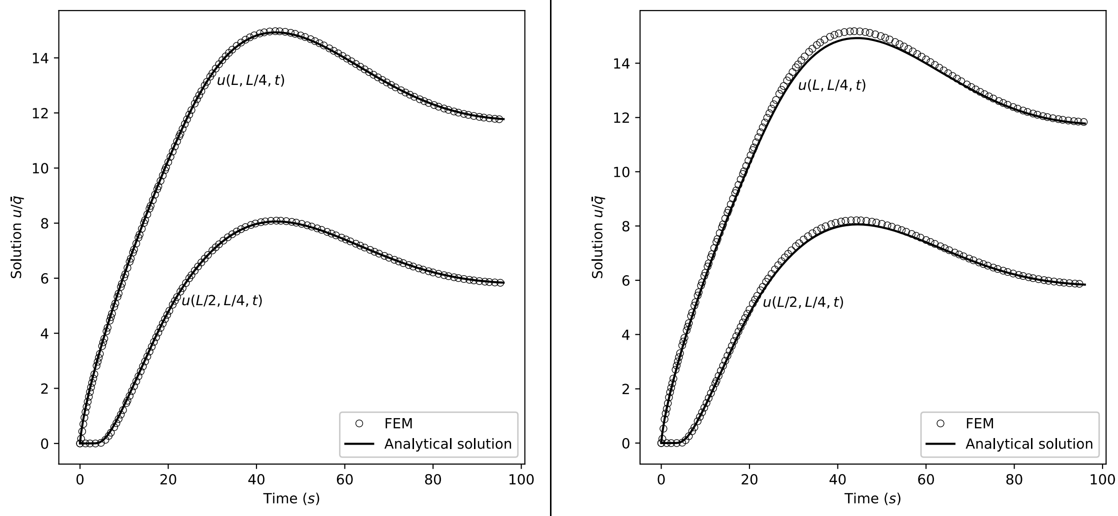

(a) FEM-WDH (α = 1.5) (b) FEM-WDN (α = 1.5)

FIGURE 7

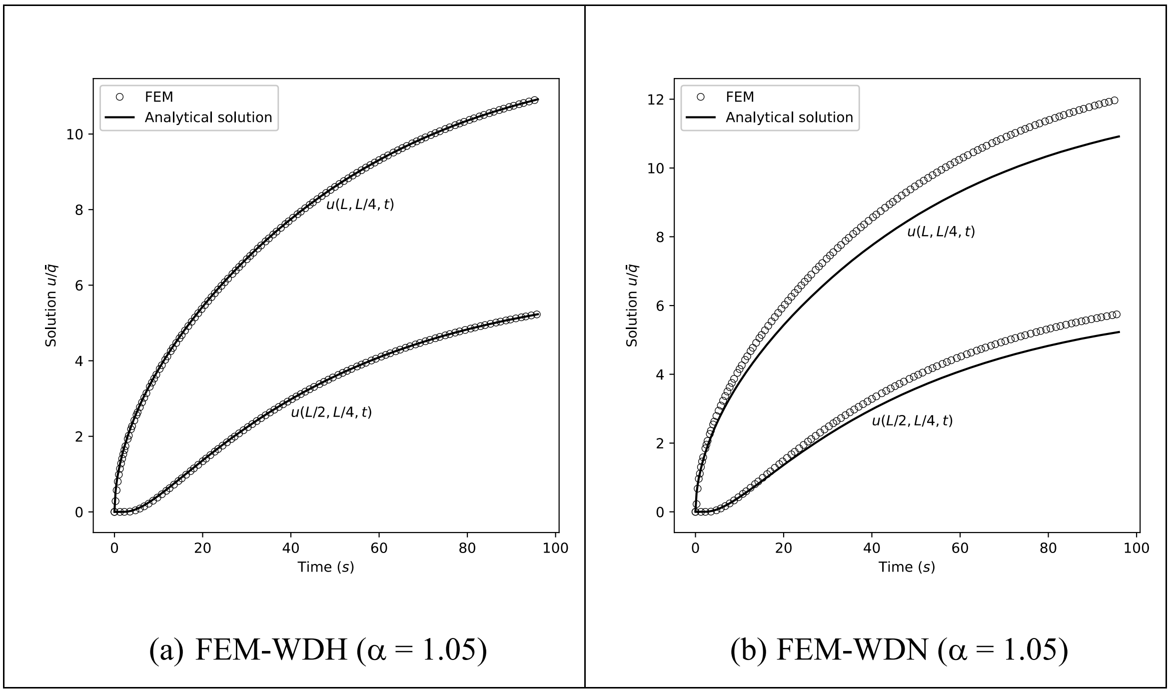

(a) FEM-WDH (α = 1.05)

(b) FEM-WDN (α = 1.05)

FIGURE 8

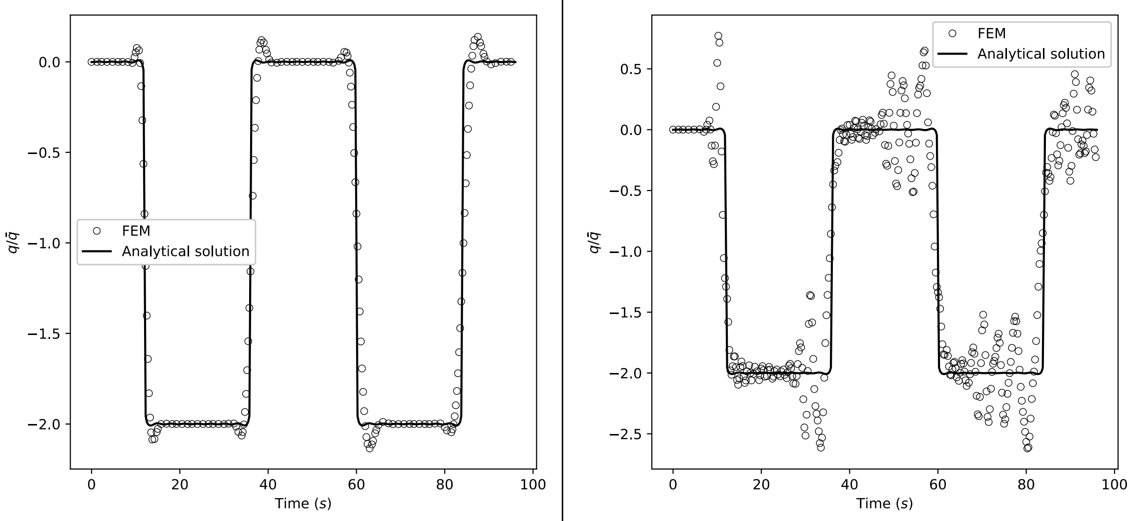

(a) FEM-WDH (α = 2.0)

(b) FEM-WDN (α = 2.0)

FIGURE 9

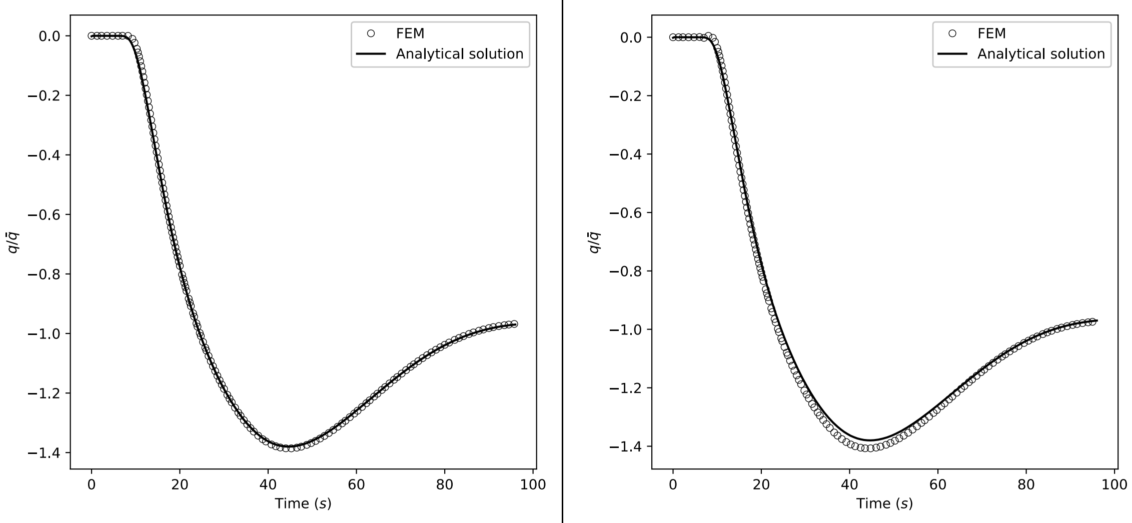

(a) FEM-WDH ($\alpha = 1.5$)

(b) FEM-WDN ($\alpha = 1.5$)

FIGURE 10

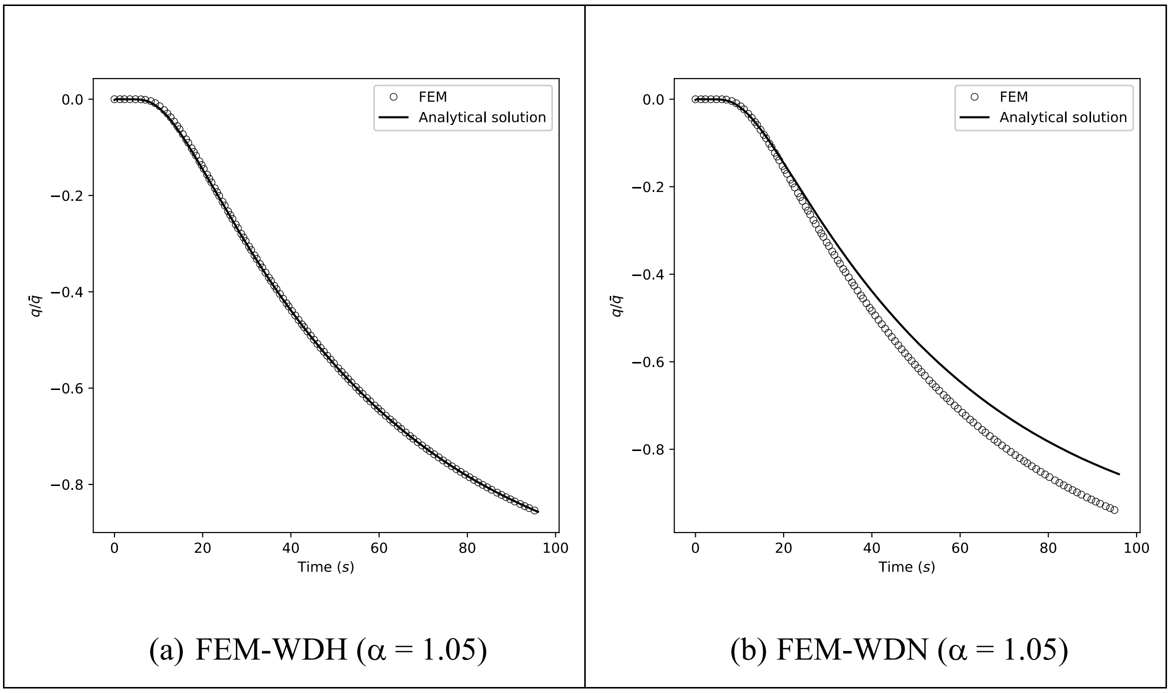
FEM
Analytical solution
$q/\bar{q}$
Time (s)
0.0
−0.2
−0.4
−0.6
−0.8
0
20
40
60
80
100
(a) FEM-WDH (α = 1.05)
(b) FEM-WDN (α = 1.05)

FIGURE 11

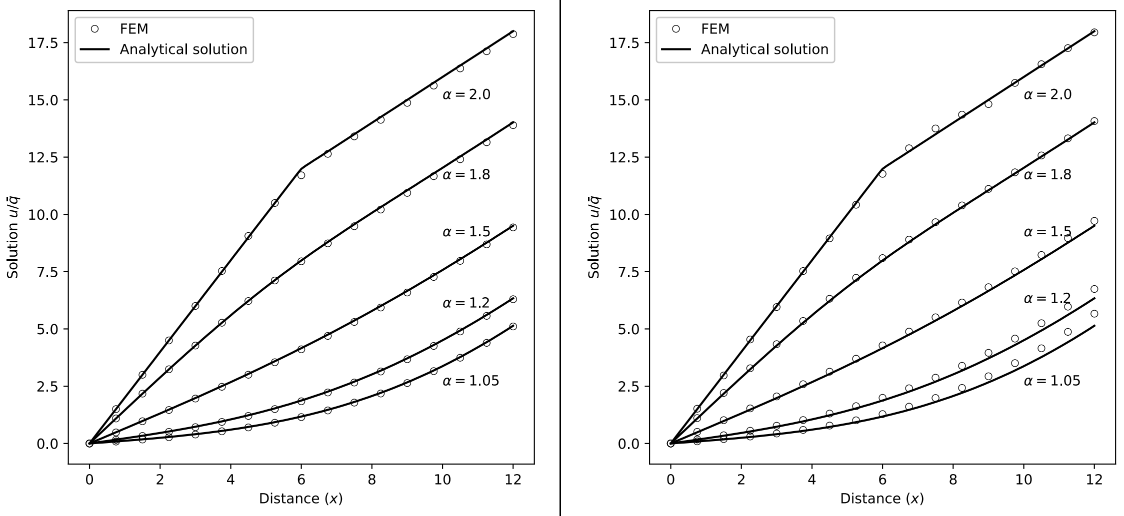

(a) FEM-WDH

(b) FEM-WDN

FIGURE 12

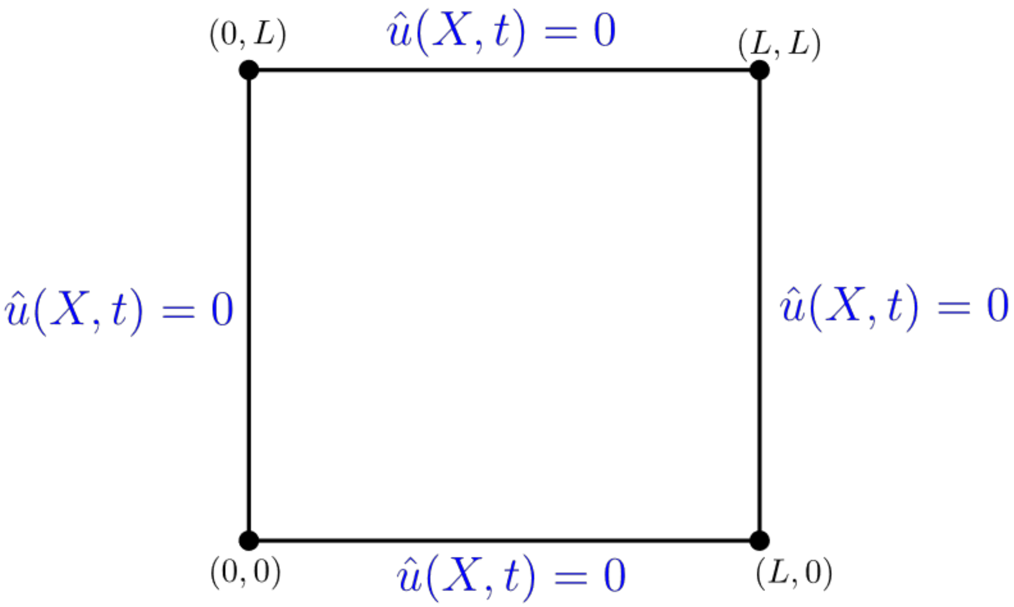

FIGURE 13

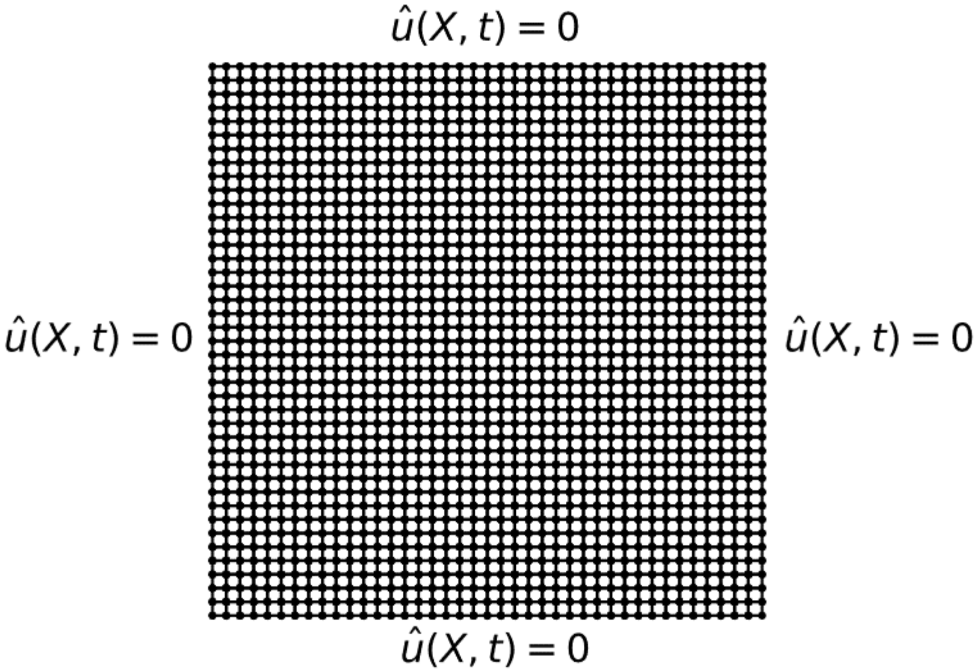

FIGURE 14

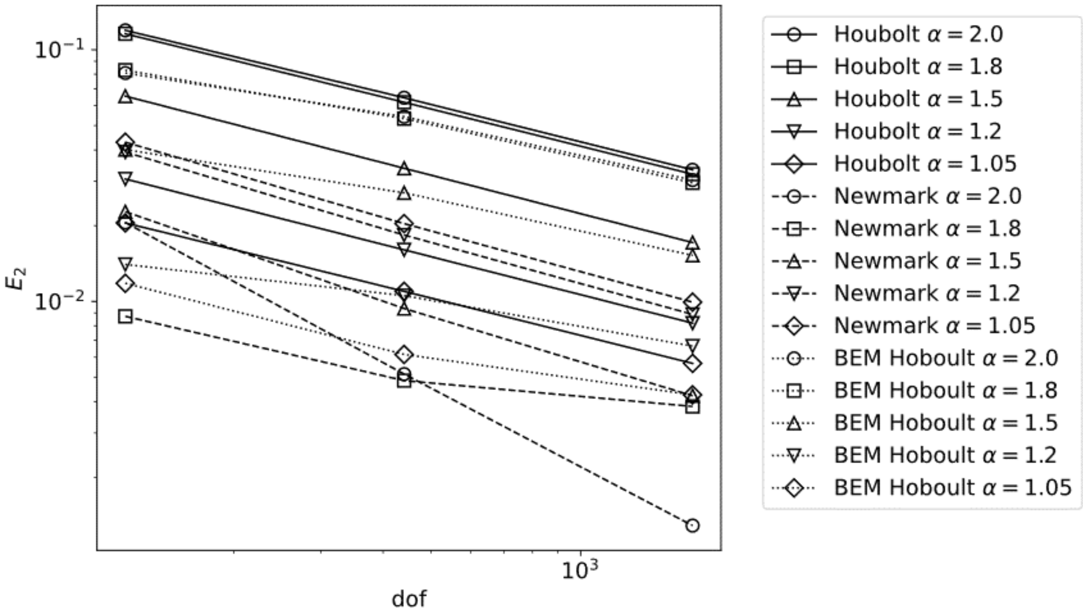

10^{-1}
10^{-2}
E_2
10^3
dof
Houbolt $\alpha = 2.0$
Houbolt $\alpha = 1.8$
Houbolt $\alpha = 1.5$
Houbolt $\alpha = 1.2$
Houbolt $\alpha = 1.05$
Newmark $\alpha = 2.0$
Newmark $\alpha = 1.8$
Newmark $\alpha = 1.5$
Newmark $\alpha = 1.2$
Newmark $\alpha = 1.05$
BEM Hoboult $\alpha = 2.0$
BEM Hoboult $\alpha = 1.8$
BEM Hoboult $\alpha = 1.5$
BEM Hoboult $\alpha = 1.2$
BEM Hoboult $\alpha = 1.05$

FIGURE 15

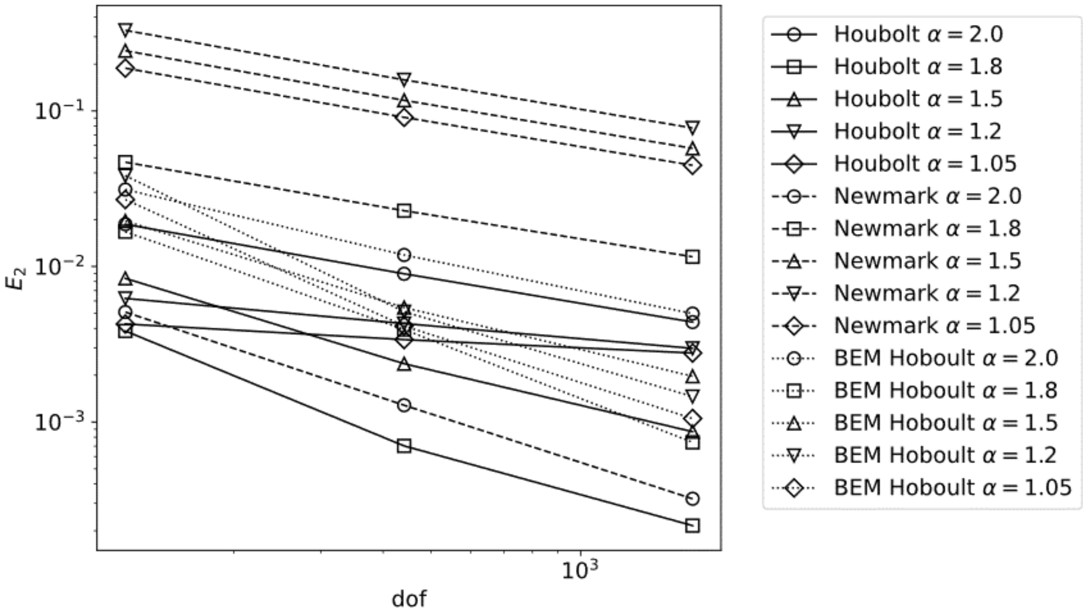

10^{-1}
10^{-2}
10^{-3}
E_2
10^3
dof
Houbolt $\alpha = 2.0$
Houbolt $\alpha = 1.8$
Houbolt $\alpha = 1.5$
Houbolt $\alpha = 1.2$
Houbolt $\alpha = 1.05$
Newmark $\alpha = 2.0$
Newmark $\alpha = 1.8$
Newmark $\alpha = 1.5$
Newmark $\alpha = 1.2$
Newmark $\alpha = 1.05$
BEM Hoboult $\alpha = 2.0$
BEM Hoboult $\alpha = 1.8$
BEM Hoboult $\alpha = 1.5$
BEM Hoboult $\alpha = 1.2$
BEM Hoboult $\alpha = 1.05$

FIGURE 16

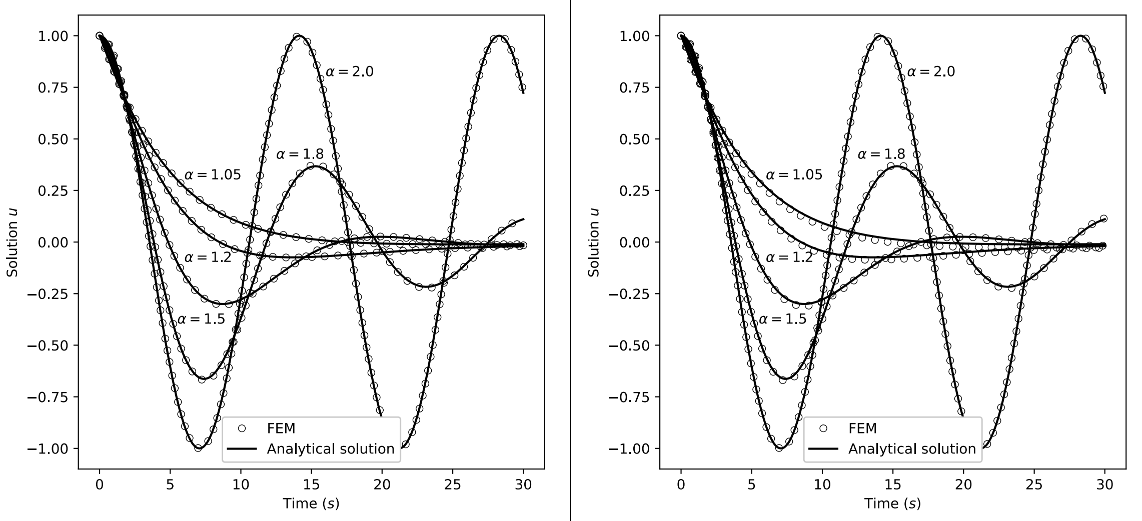

(a) FEM-WDH

(b) FEM-WDN

FIGURE 17

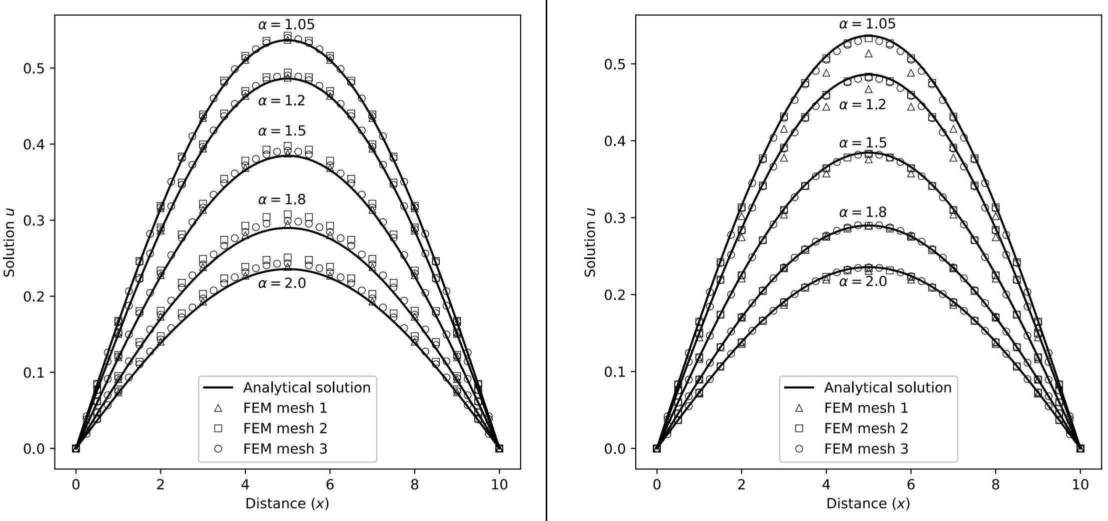

(a) FEM-WDH (b) FEM-WDN

FIGURE 18

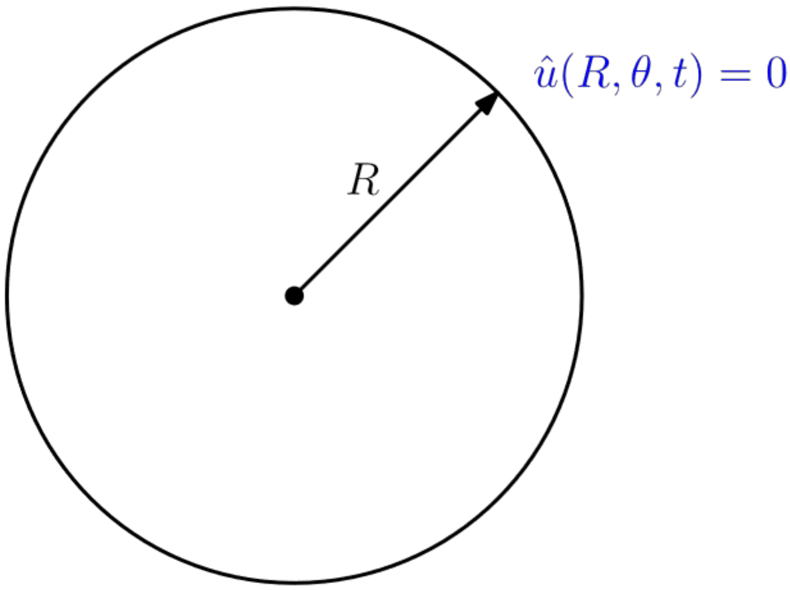

FIGURE 19

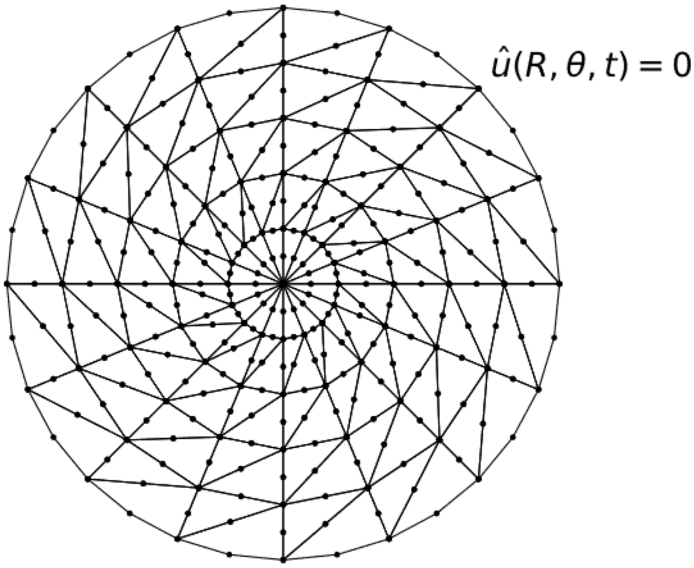

FIGURE 20

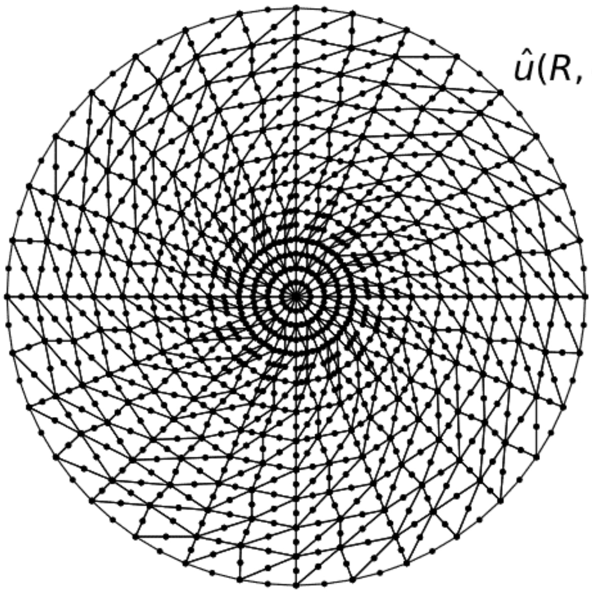

FIGURE 21

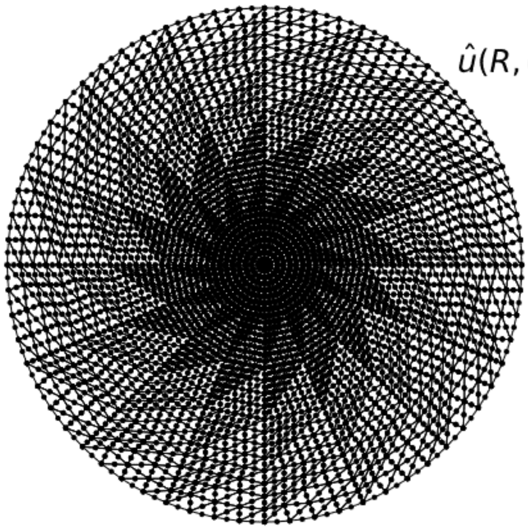

FIGURE 22

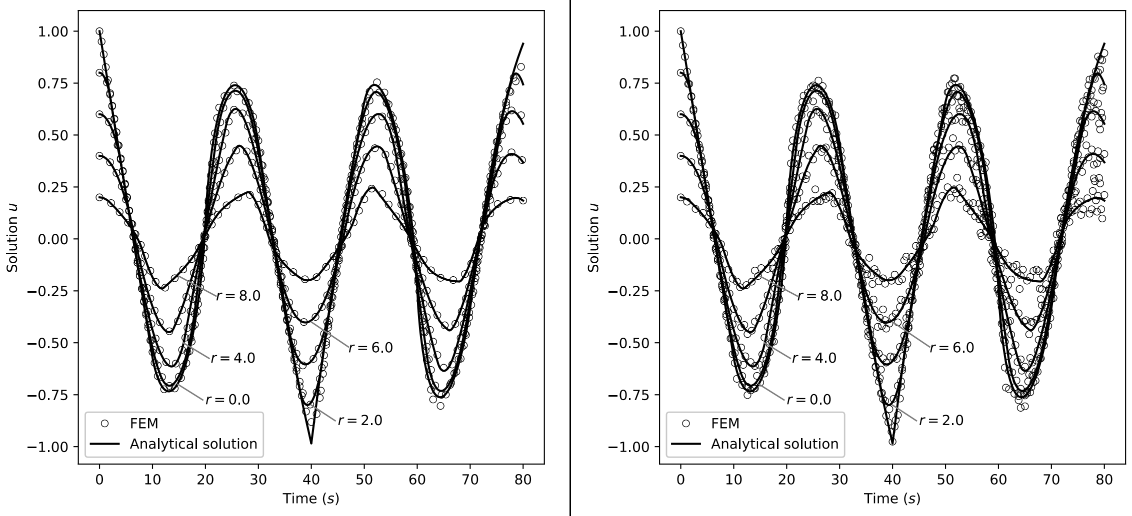

(a) FEM-WDH (α = 2.0) (b) FEM-WDN (α = 2.0)

FIGURE 23

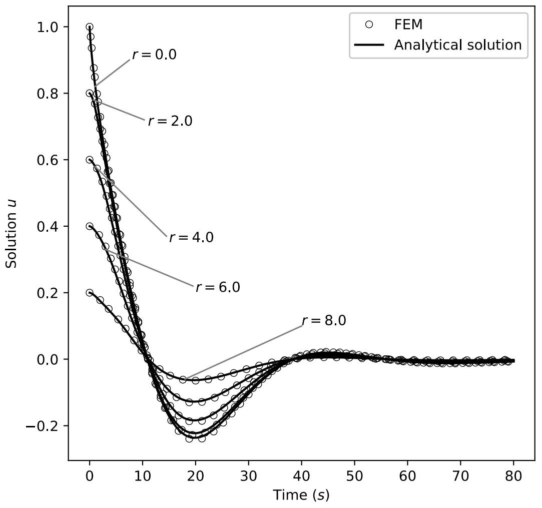

(a) FEM-WDH (α = 1.5)

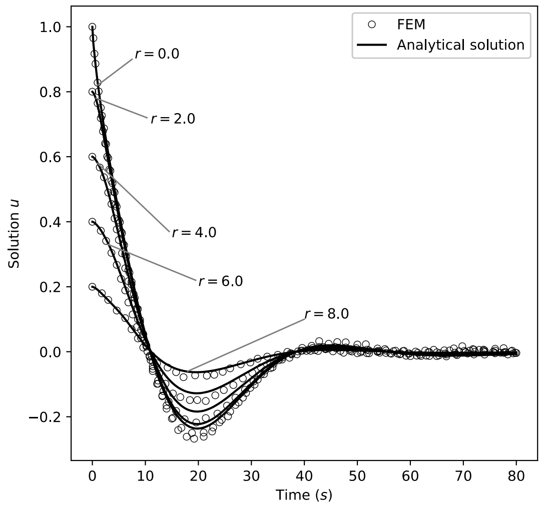

(b) FEM-WDN (α = 1.5)

FIGURE 24

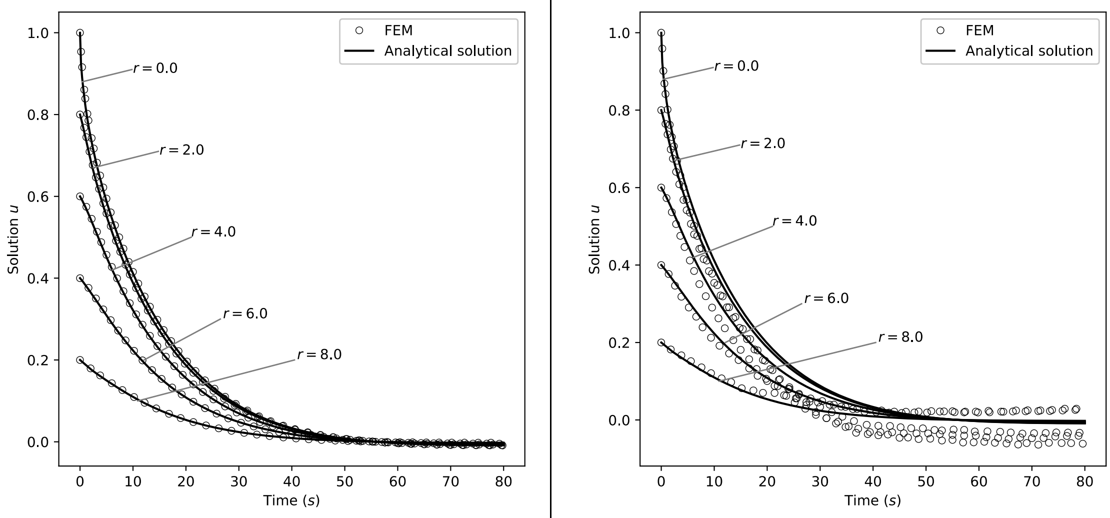

(a) FEM-WDH (α = 1.05) (b) FEM-WDN (α = 1.05)

FIGURE 25

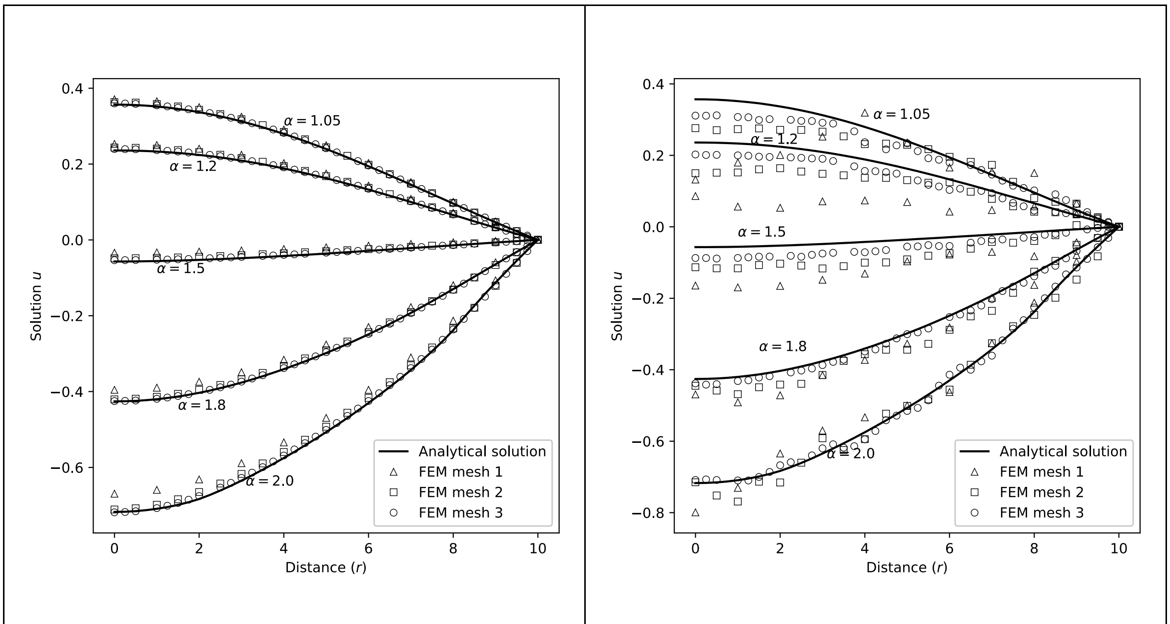

(a) FEM-WDH

(b) FEM-WDN

FIGURE 26

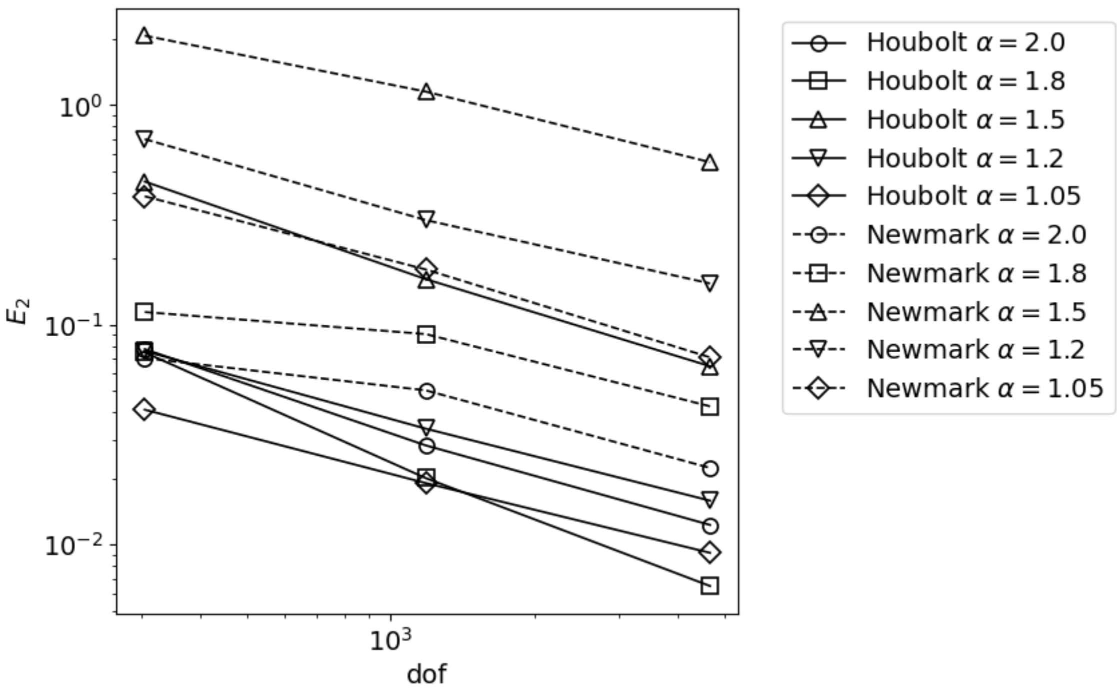
10^0
10^{-1}
10^{-2}
E_2
10^3
dof
Houbolt $\alpha = 2.0$
Houbolt $\alpha = 1.8$
Houbolt $\alpha = 1.5$
Houbolt $\alpha = 1.2$
Houbolt $\alpha = 1.05$
Newmark $\alpha = 2.0$
Newmark $\alpha = 1.8$
Newmark $\alpha = 1.5$
Newmark $\alpha = 1.2$
Newmark $\alpha = 1.05$

FIGURE 27

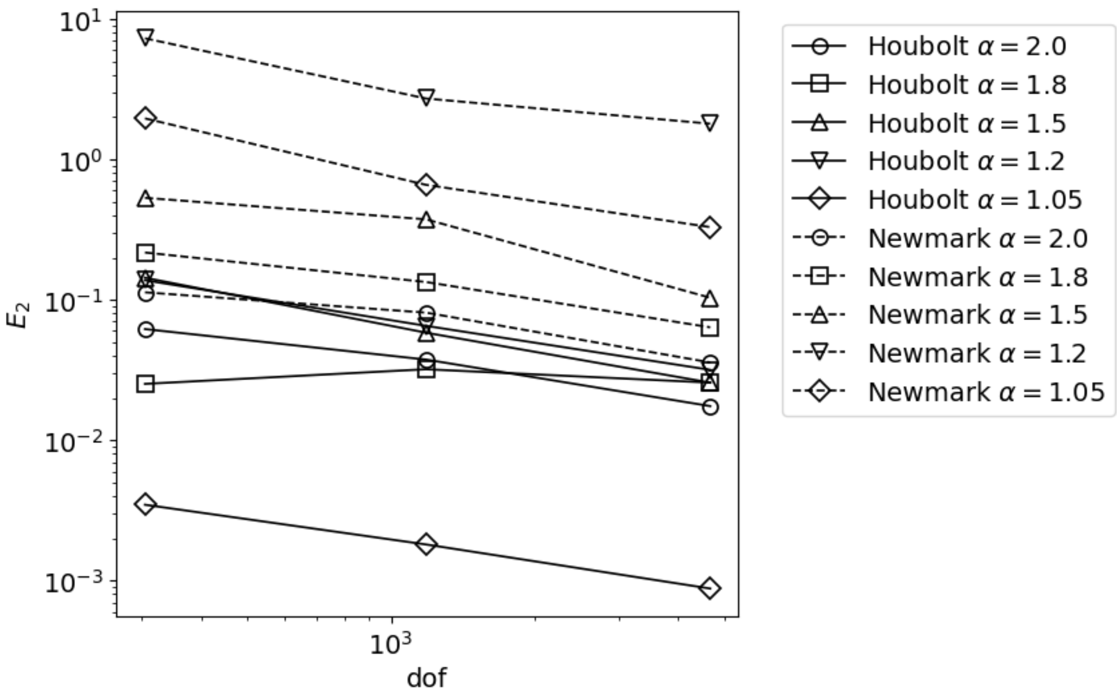
10^1
10^0
10^{-1}
10^{-2}
10^{-3}
E_2
10^3
dof
Houbolt $\alpha = 2.0$
Houbolt $\alpha = 1.8$
Houbolt $\alpha = 1.5$
Houbolt $\alpha = 1.2$
Houbolt $\alpha = 1.05$
Newmark $\alpha = 2.0$
Newmark $\alpha = 1.8$
Newmark $\alpha = 1.5$
Newmark $\alpha = 1.2$
Newmark $\alpha = 1.05$

FIGURE 28